Proceedings of the 29th Annual International
Conference of the IEEE EMBS
Cité Internationale, Lyon, France
August 23-26, 2007.

SaP2C1.1

Optimal Operating Frequency in Wireless Power Transmission for Implantable Devices

Ada S. Y. Poon, Stephen O'Driscoll, and Teresa H. Meng

Abstract— This paper examines short-range wireless powering for implantable devices and shows that existing analysis techniques are not adequate to conclude the characteristics of power transfer efficiency over a wide frequency range. It shows, theoretically and experimentally, that the optimal frequency for power transmission in biological media can be in the GHz-range while existing solutions exclusively focus on the MHz-range. This implies that the size of the receive coil can be reduced by 10^4 times which enables the realization of fully integrated implantable devices.

I. INTRODUCTION

Implantable medical devices (IMDs) are useful for health monitoring, disease prevention, and biomimetic prosthesis. In recent years, the power consumption of these devices has been reduced dramatically. For example, cochlear implants can run on a power level of 1 mW, and pacemakers can run on power levels ranging from 10 μW to 1 mW. However, the wireless interface for both power and data transmission, usually through inductive coupling, remains bulky and therefore is not suitable to embed in the implant. Its relatively large size is a result of the common belief that lower operating frequency yields higher power transfer efficiency. Most of these wireless interfaces operate below 20 MHz [1]–[3]. Quasi-static analysis was sufficient to analyze these wireless links [4]–[8]. The quasi-static approximation works well at low frequency. The conclusion drawn from this approximation does not favor the operation at higher frequencies which is also the source of the common belief.

In this paper, we remove the quasi-static approximation, and show that the power transfer efficiency exhibits certain optimal frequency in the GHz-range by carrying out the full-wave analysis taking into account the relaxation loss of biological tissue as well as the layered structure of tissue. Higher operating frequency reduces the size of the receive antenna. To deliver the same amount of power, a 10^4 times smaller antenna can be used at 1 GHz than that at 10 MHz without increasing tissue absorption. This gives a lot of room for practical realization of integrating the receive antenna with the rest of the implant circuits for a complete implant-on-chip solution. Not only is the conventional analysis technique for wireless powering inadequate, the design methodology based on inductive coupling [9]–[14] cannot be applied directly. We

will show that generalized matching network should be used as opposed to simple RLC tuning circuits. Finally, we verify the analytical results through electromagnetic simulation and experiment with real biological tissue.

In the following, we use boldface letters for vectors and boldface letters with a bar $\bar{\mathbf{G}}$ for matrices. For a vector $\mathbf{v}$, v denotes its magnitude and $\hat{\mathbf{v}}$ is a unit vector denoting its direction. $\bar{\mathbf{I}}$ is the identity matrix. $(\cdot)^*$ denotes the conjugate operation. For a complex number z, $\mathrm{Re}\,z$ and $\mathrm{Im}\,z$ denote the real and the imaginary parts respectively.

II. QUASI-STATIC VS. FULL-WAVE ANALYSES

We will first re-examine the conventional analysis technique used in the wireless interface for implantable devices, and illustrate the origin of the common belief that lower frequency is better. Then we will perform full-wave analysis and illustrate an opposite conclusion. Since coils are usually used in these wireless interfaces, it is more convenient to consider magnetic current density $\mathbf{J}_m$ as sources in a lossy homogeneous medium. The inhomogeneous counterpart will be detailed in Section IV. The Maxwell's equations are

$$\nabla \times \mathbf{H} = -i\omega\epsilon_0\epsilon_r\mathbf{E} + \sigma\mathbf{E} \tag{1a}$$
$$\nabla \times \mathbf{E} = i\omega\mu_0\mathbf{H} - \mathbf{J}_m \tag{1b}$$

where ϵ_r is the relative permittivity of the biological medium. The displacement current, $-i\omega\epsilon_0\epsilon_r\mathbf{E}$, is small at low frequency. Quasi-static approximation refers to the neglect of this current.

A. Quasi-static Approximation

Neglecting the displacement current, solutions to (1) can be expressed in integral forms as

$$\mathbf{H}(\mathbf{x}) = -\sigma \int \bar{\mathbf{G}}_m(\mathbf{x} - \mathbf{x}') \cdot \mathbf{J}_m(\mathbf{x}')\,d^3x' \tag{2a}$$

$$\mathbf{E}(\mathbf{x}) = \int \bar{\mathbf{G}}_e(\mathbf{x} - \mathbf{x}') \cdot \mathbf{J}_m(\mathbf{x}')\,d^3x' \tag{2b}$$

where the corresponding Green functions are

$$\bar{\mathbf{G}}_m(\mathbf{r}) = \frac{e^{-\frac{(1-i)}{\delta}r}}{4\pi r}\left[(\bar{\mathbf{I}} - \hat{\mathbf{r}}\hat{\mathbf{r}}) + \frac{\delta}{(1-i)r}(\bar{\mathbf{I}} - 3\hat{\mathbf{r}}\hat{\mathbf{r}}) \right. $$
$$\left. + \frac{\delta^2}{(1-i)^2r^2}(\bar{\mathbf{I}} - 3\hat{\mathbf{r}}\hat{\mathbf{r}})\right] \tag{3a}$$

$$\bar{\mathbf{G}}_e(\mathbf{r}) = \frac{(1-i)\,e^{-\frac{(1-i)}{\delta}r}}{4\pi\delta r}\left[1 + \frac{\delta}{(1-i)r}\right]\hat{\mathbf{r}} \times \bar{\mathbf{I}} \tag{3b}$$

and $\delta := \sqrt{\frac{2}{\omega\mu_0\sigma}}$ is the skin depth. Suppose the transmit and the receive magnetic current densities are $\mathbf{J}_{m1}$ and $\mathbf{J}_{m2}$ respectively. Then, the power transferred to the implant is

$$P_r = \frac{1}{2}\,\mathrm{Re}\int \mathbf{J}_{m2}^*(\mathbf{x}) \cdot \mathbf{H}(\mathbf{x})\, d\mathbf{x} \tag{4a}$$

$$= -\frac{\sigma}{2}\,\mathrm{Re}\iint \mathbf{J}_{m2}^*(\mathbf{x}) \cdot \bar{\mathbf{G}}_m(\mathbf{x} - \mathbf{x}') \cdot \mathbf{J}_{m1}(\mathbf{x}')\, d\mathbf{x}' d\mathbf{x} \tag{4b}$$

and the tissue absorption is

$$P_{\mathrm{loss}} = \frac{\sigma}{2}\int |\mathbf{E}(\mathbf{x})|^2\, d\mathbf{x} \tag{5a}$$

$$= \frac{\sigma}{2}\int \left| \int \bar{\mathbf{G}}_e(\mathbf{x} - \mathbf{x}') \cdot \mathbf{J}_{m1}(\mathbf{x}')\, d\mathbf{x}' \right|^2 d\mathbf{x} \tag{5b}$$

The efficiency is defined as $\eta := \frac{P_r}{P_{\mathrm{loss}}}$. Finally, the magnetic current density on the implant $\mathbf{J}_{m2}$ is induced by the incident magnetic field so $\mathbf{J}_{m2}$ must relate to $\mathbf{J}_{m1}$.

To get the insight, we consider point sources. As magnetic current density $\mathbf{J}_m$ relates to magnetic moment density $\mathbf{M}$ by $\mathbf{J}_m = -i\omega\mu_0\mathbf{M}$, the source functions can be written as

$$\mathbf{J}_{mn}(\mathbf{x}) = -i\omega\mu_0 M_n\, \mathbf{m}_n\, \delta(\mathbf{x} - \mathbf{x}_n) \qquad n = 1, 2$$

where $\mathbf{x}_1$ and $\mathbf{x}_2$ are locations of the transmit and the receive magnetic dipoles respectively. The transmit dipole is oriented along $\mathbf{m}_1$ with magnetic moment M_1 whereas the receive dipole is oriented along $\mathbf{m}_2$ with magnetic moment M_2. The magnetic field incident on the receive dipole is $\mathbf{H}(\mathbf{x}_2) \cdot \mathbf{m}_2$, and the rate of change of the magnetic flux incident on it is $-i\omega\mu_0\mathbf{H}(\mathbf{x}_2) \cdot \mathbf{m}_2$ which should be proportional to the induced magnetic moment on the receiver:

$$M_2 = \frac{i\omega\mu_0\mathbf{H}(\mathbf{x}_2) \cdot \mathbf{m}_2}{\zeta} \tag{6}$$

where ζ is the proportionality constant. In Section V, we will show that ζ is the input impedance of the implant coil divided by the square of the coil area. Now, the receive power and the tissue absorption can be written as

$$P_r = \frac{(\sigma\omega^2\mu_0^2)^2\,\mathrm{Re}\frac{1}{\zeta^*}}{2}|M_1|^2 \big|\mathbf{m}_2^* \cdot \bar{\mathbf{G}}_m(\mathbf{x}_2 - \mathbf{x}_1) \cdot \mathbf{m}_1\big|^2 \tag{7a}$$

$$P_{\mathrm{loss}} = \frac{\sigma\omega^2\mu_0^2}{2}|M_1|^2\mathbf{m}_1^\dagger\left[\int \bar{\mathbf{G}}_e^*(\mathbf{x} - \mathbf{x}_1) \cdot \bar{\mathbf{G}}_e(\mathbf{x} - \mathbf{x}_1)\, d\mathbf{x}\right]\mathbf{m}_1 \tag{7b}$$

Note the ratio, equal to the efficiency, is independent of M_1.

Suppose the transmit dipole is at the origin and the receive dipole is at $-d\hat{\mathbf{z}}$. The dipole can be decomposed into a vertical magnetic dipole (VMD) and a horizontal magnetic dipole (HMD). From (3), the transmit VMD only couples to the receive VMD. Similarly, the transmit HMD only couples to the receive HMD that orients in parallel with the transmit dipole. Therefore, we will consider two orientations: face-to-face and edge-to-edge. In the face-to-face orientation, both dipoles are vertically oriented as shown in Fig. 1. Suppose
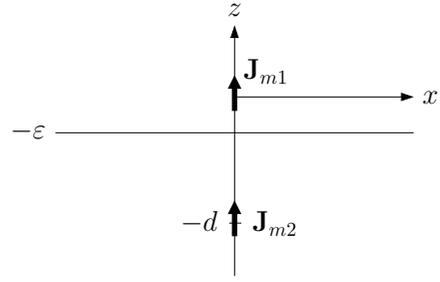

Fig. 1. The transmit and the implant coils are oriented face-to-face.

the integration in computing the tissue absorption is over the half space $z < -\varepsilon$. The efficiency becomes

$$\eta_{\mathrm{qs}}^{\mathrm{f2f}} = \frac{8\varepsilon\,\mathrm{Re}\frac{1}{\zeta^*}}{\pi\sigma d^6}\,\frac{e^{-\frac{2d}{\delta}}\left(1 + \frac{2d}{\delta} + \frac{2d^2}{\delta^2}\right)}{e^{-\frac{2\varepsilon}{\delta}}\left(1 - \frac{2\varepsilon}{3\delta} + \frac{2\varepsilon^2}{3\delta^2} - \frac{4\varepsilon^3}{3\delta^3}\right) - \mathrm{Ei}\!\left(-\frac{2\varepsilon}{\delta}\right)\frac{8\varepsilon^4}{3\delta^4}}$$

where $\mathrm{Ei}(\cdot)$ is the exponential integral. In the edge-to-edge orientation, both dipoles are horizontally oriented and in parallel. The efficiency is given by

$$\eta_{\mathrm{qs}}^{\mathrm{e2e}} = \frac{4\varepsilon\,\mathrm{Re}\frac{1}{\zeta^*}}{3\pi\sigma d^6}\,\frac{e^{-\frac{2d}{\delta}}\left(1 + \frac{2d}{\delta} + \frac{2d^2}{\delta^2} + \frac{4d^3}{\delta^3} + \frac{4d^4}{\delta^4}\right)}{e^{-\frac{2\varepsilon}{\delta}}\left(1 + \frac{2\varepsilon}{9\delta} - \frac{2\varepsilon^2}{9\delta^2} + \frac{4\varepsilon^3}{9\delta^3}\right) + \mathrm{Ei}\!\left(-\frac{2\varepsilon}{\delta}\right)\frac{8\varepsilon^4}{9\delta^4}}$$

Now, let us look at two regimes of frequency region:

1) *DC.* When $\omega = 0$,

$$\eta_0^{\mathrm{f2f}} = \frac{8\varepsilon\,\mathrm{Re}\frac{1}{\zeta^*}}{\pi\sigma d^6} \qquad \eta_0^{\mathrm{e2e}} = \frac{4\varepsilon\,\mathrm{Re}\frac{1}{\zeta^*}}{3\pi\sigma d^6} \tag{8}$$

Efficiencies depend only on the geometry of the system and are independent of frequency.

2) *High frequency.* When $\omega \gg 1$, the skin depth $\delta \ll 1$. Assume that the spacing between the transmit coil and the tissue volume decreases as the skin depth decreases, and is related by $\varepsilon \propto \delta^2$. The asymptotic efficiencies are given by

$$\eta_{\mathrm{qs}}^{\mathrm{f2f}} = \frac{16\,\mathrm{Re}\frac{1}{\zeta^*}}{\pi\sigma d^4}\,e^{-2d/\delta} + o(e^{-2d/\delta}) \tag{9a}$$

$$\eta_{\mathrm{qs}}^{\mathrm{e2e}} = \frac{16\,\mathrm{Re}\frac{1}{\zeta^*}}{3\pi\sigma d^4}\,\frac{d^2}{\delta^2}\,e^{-2d/\delta} + o(e^{-2d/\delta}) \tag{9b}$$

as $\delta \to 0$. In the face-to-face orientation, η^{f2f} *decreases exponentially with increasing frequency. In the edge-to-edge orientation,* η^{e2e} *first increases with frequency and after reaching the optimal frequency, it also decreases exponentially with increasing frequency.*

As a whole, the efficiency decreases exponentially with increasing frequency. Therefore, it is commonly believed that wireless powering is preferred at low frequency.

B. Full-wave Analysis

Including the displacement current, solutions to (1) can be obtained from (2) by the following substitutions: $\sigma \to -i\omega\epsilon$ and $\frac{1-i}{\delta} \to -ik$ where $k^2 := \omega^2\mu\epsilon$. Similarly, efficiencies in the face-to-face and the edge-to-edge orientations are derived and the asymptotic results in the two frequency regimes are:

5674

1) *DC.* When $\omega = 0$,

$$\eta_0^{\text{f2f}} = \frac{8\varepsilon \operatorname{Re} \frac{1}{\zeta^*}}{\pi\sigma d^6} \qquad \eta_0^{\text{e2e}} = \frac{4\varepsilon \operatorname{Re} \frac{1}{\zeta^*}}{3\pi\sigma d^6} \qquad (10)$$

which agrees with the quasi-static analysis.

2) *High frequency.* When $\omega \gg 1$, we have

$$k = \omega\sqrt{\mu_0\epsilon_0\epsilon_r} + i\frac{\sigma}{2}\sqrt{\frac{\mu_0}{\epsilon_0\epsilon_r}} + o(1) \qquad (11)$$

as $\omega \to \infty$. Assuming $\varepsilon \propto |k|^{-2}$ and defining the low-frequency skin depth $\delta_0 := \frac{2}{\sigma}\sqrt{\frac{\epsilon_0\epsilon_r}{\mu_0}}$, the efficiencies can be expressed as

$$\eta^{\text{f2f}} = \frac{8\operatorname{Re}\frac{1}{\zeta^*}}{\pi\sigma d^4}\frac{e^{-2d/\delta_0}}{1 + \frac{4}{3}\delta_0} + o(1) \qquad (12a)$$

$$\eta^{\text{e2e}} = \frac{4\operatorname{Re}\frac{1}{\zeta^*}}{3\pi\sigma d^4}\frac{\omega^2\mu_0\epsilon_0\epsilon_r d^2\, e^{-2d/\delta_0}}{1 + \frac{8}{9}\delta_0} + o(\omega^2) \quad (12b)$$

as $\omega \to \infty$. In contrast to those obtained from the quasi-static analysis, η^{f2f} *remains approximately constant while η^{e2e} increases quadratically with frequency.*

As a whole, the efficiency increases with frequency. The misconception in the common belief is due to the use of a low-frequency approximation technique to conclude the behavior at high frequency.

III. RELAXATION LOSS

The efficiency would not increase indefinitely with frequency. At high frequency, there are loss mechanisms other than conduction current. The dominant mechanism is the relaxation loss [15] – the change in the polarization cannot follow the applied electric field, and the time lag between the electric field and the polarization incurs an energy loss. Consequently, there will be an optimal operating frequency. We are interested in finding where it is, in the MHz-range or in the GHz-range. A relaxation model is therefore needed.

Dielectric relaxation is often modeled by a frequency-dependent permittivity. Debye relaxation model and its variants are popular models for biological media. In this relaxation model, the time scale of the delay is characterized by a relaxation time constant, τ. The relative permittivity of the medium is expressed as a function of frequency:

$$\epsilon_r(\omega) = \epsilon_\infty + \frac{\epsilon - \epsilon_\infty}{1 - i\omega\tau} + i\frac{\sigma}{\omega\epsilon_0} \qquad (13)$$

In the expression, ϵ_∞ is the relative permittivity at frequencies where $\omega\tau \gg 1$, while ϵ is the relative permittivity at $\omega\tau \ll 1$. In the frequency region where $\omega\tau \ll 1$, the relative permittivity is approximately equal to

$$\epsilon_r(\omega) \approx \epsilon + \frac{i}{\omega\epsilon_0}\left(\omega^2\tau\epsilon_0\Delta\epsilon + \sigma\right) \qquad (14)$$

where $\Delta\epsilon = \epsilon - \epsilon_\infty$.

The asymptotic efficiencies can be obtained from (12) by the following substitutions: $\epsilon_r \to \epsilon$ and $\sigma \to \sigma + \omega^2\tau\epsilon_0\Delta\epsilon$.

TABLE I

SUMMARY OF THE LOWER BOUND ON THE OPTIMAL FREQUENCY
$f_{\text{OPT,LB}}$ AND THE UPPER BOUND ON THE WAVELENGTH $\lambda_{\text{OPT,UB}}$.

Tissue type	Bounds $f_{\text{opt,LB}}$	$\lambda_{\text{opt,UB}}$	$d = 1.5$ cm f_{opt}	λ_{opt}
Skin (wet)	0.8 GHz	5.5 cm	2.0 GHz	2.3 cm
Fat	1.2 GHz	1.0 cm	3.7 GHz	3.5 cm
Muscle	1.2 GHz	3.3 cm	2.2 GHz	1.9 cm
Bone (cancellous)	0.7 GHz	9.1 cm	1.8 GHz	3.7 cm
Brain (grey matter)	1.0 GHz	4.3 cm	2.0 GHz	2.1 cm

They are

$$\eta^{\text{f2f}} = \frac{8\operatorname{Re}\frac{1}{\zeta^*}}{\pi\sigma d^4}\frac{e^{-2d/\delta_0(1+\omega^2\tau\epsilon_0\Delta\epsilon/\sigma)}}{1 + \omega^2\tau\epsilon_0\Delta\epsilon/\sigma + \frac{4}{3}\delta_0} + o(\omega^{-2}) \quad (15a)$$

$$\eta^{\text{e2e}} = \frac{4\operatorname{Re}\frac{1}{\zeta^*}}{3\pi\sigma d^4}\frac{\omega^2\mu_0\epsilon_0\epsilon d^2\, e^{-2d/\delta_0(1+\omega^2\tau\epsilon_0\Delta\epsilon/\sigma)}}{1 + \omega^2\tau\epsilon_0\Delta\epsilon/\sigma + \frac{8}{9}\delta_0} + o(1) \tag{15b}$$

as $\omega \to \infty$. When $\omega \ll \frac{\sigma}{(\omega\tau)\epsilon_0\Delta\epsilon}$, η^{f2f} remains approximately constant and η^{e2e} increases quadratically with frequency. However, when $\omega \gg \frac{\sigma}{(\omega\tau)\epsilon_0\Delta\epsilon}$, both η^{f2f} and η^{e2e} decrease exponentially with frequency. As $\omega\tau \ll 1$, we expect the optimal frequency to be large. The first term in η^{e2e} is maximized when

$$\omega_{\text{opt}} = \sqrt{\frac{\sigma(1 + 8\delta_0/9)}{2\tau\epsilon_0\Delta\epsilon}\left(\sqrt{1 + \frac{2\delta_0/d}{1 + 8\delta_0/9}} - 1\right)} \quad (16)$$

Gabriel et al. have experimentally characterized the dielectric properties of different kind of body tissue [16]. As muscle is one of the most widely reported tissue, let us look into muscle first. Over the frequency range 2.8 MHz $\ll \omega \ll$ 140 GHz, muscle has the following dielectric properties: $\tau = 7.23$ ps, $\epsilon_\infty = 4$, $\epsilon = 54$, and $\sigma = 0.5$ S/m. Suppose the transmit-receive separation is smaller than the low-frequency skin depth, that is, $d < \delta_0$. Then, the optimal frequency is lower-bounded by 1.2 GHz. Table I tabulates the lower bound on the optimal frequency and the corresponding upper bound on the wavelength for five different kinds of biological tissue. It also includes the exact values when $d = 1.5$ cm. We can conclude that the *optimal frequency is in the GHz-range.*

As the receive power is proportional to $\frac{\omega^4}{\zeta^*}$ in the face-to-face orientation and $\frac{\omega^6}{\zeta^*}$ in the edge-to-edge orientation, and $\frac{1}{\zeta}$ is proportional to the square of the area of the receive coil, the size of the receive coil can be reduced by 10^4 times in the face-to-face and 10^6 times in the edge-to-edge without incurring more tissue absorption by operating in the GHz-range as opposed to in the MHz-range

IV. INHOMOGENEOUS MEDIUM

We include the air-tissue interface and follow the approach in [17, Section 2.3] to calculate the electromagnetic fields across the interface. To demonstrate the optimal frequencies
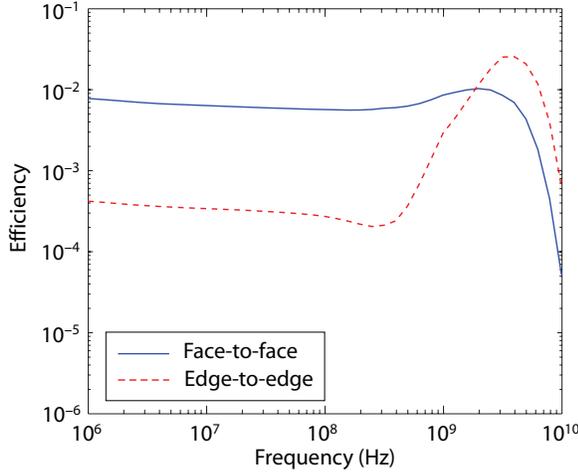
5675

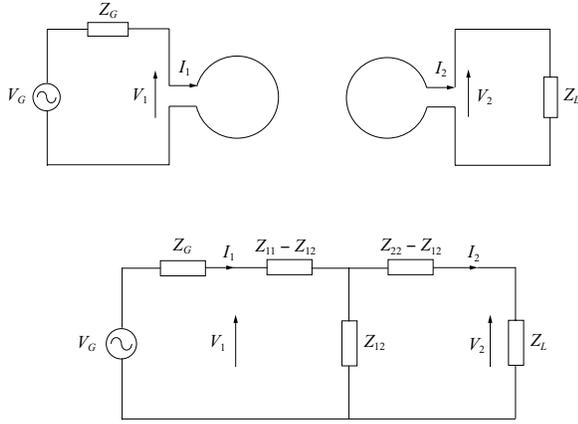Fig. 2. Efficiencies versus frequency across air-muscle interface.

Fig. 3. Equivalent circuit for a single transmit and single receive coil system.

are close to the predicted ones, we consider an example with link parameters: $d = 1.5$ cm, $\varepsilon = 1$ mm, and $\zeta = (0.002)^{-4}\,\Omega/\text{m}^4$. Furthermore, we consider the air-muscle interface and use parameters from [16] for the 4 Cole-Cole relaxation model, a variant of the Debye relaxation model. Fig. 2 plots the efficiency versus frequency. In the face-to-face orientation, η^{f2F} exhibits an optimal frequency at 2 GHz but the peak is gentle. In the edge-to-edge orientation, the optimal frequency is much sharper and is 3.5 GHz. The efficiency is slightly higher in the edge-to-edge than in the face-to-face. The results reinforce that the optimal operating frequency is in the GHz-range.

V. EQUIVALENT CIRCUITS

Up to this point, the interaction between the incident field and the induced magnetic current density is encapsulated by the proportionality constant ζ. We will find this interaction by the equivalent circuit. The equivalent circuit for a system with a single transmit and a single receive coil is shown in Fig. 3 assuming the system is reciprocal. The receive current

and the power transferred to the receiver can be written as

$$I_2 = \frac{Z_{12}}{Z_{22} + Z_L} I_1 \tag{17a}$$

$$P_{1\to2} = \frac{1}{2}(Z_{22} + Z_L)\left|\frac{Z_{12}}{Z_{22} + Z_L}\right|^2 |I_1|^2 \tag{17b}$$

Define A_1 as the area of the transmit coil and A_2 as the area of the receive coil. Equating I_2 with M_2/A_2 in (6) and $P_{1\to2}$ with P_r in (7a) yield

$$\zeta = \frac{Z_{22} + Z_L}{A_2^2} \tag{18a}$$

$$Z_{12} = i\omega\mu_0 k^2 A_1 A_2\, \mathbf{m}_2^* \cdot \bar{\mathbf{G}}_m(\mathbf{x}_2 - \mathbf{x}_1) \cdot \mathbf{m}_1 \tag{18b}$$

Thus, ζ equals to the input impedance of the receiver, $Z_{22} + Z_L$, divided by A_2^2. As the power transfer efficiency depends on ζ and ζ depends on the load impedance Z_L, ζ should also be a function of frequency. The frequency dependence can be found by finding the load impedance that gives the optimal power gain at each frequency.

In order to find the optimal power gain, we need to define the impedances Z_{11} and Z_{22}. The sum $\frac{1}{2}\,\text{Re}(Z_{11}|I_1|^2 + Z_{22}|I_2|^2)$ is the total dissipation power which includes tissue absorption due to the sum of incident field from the transmit coil and scattered field from the receive coil, ohmic loss in both coils, and radiated power. As mentioned in [18] and subsequent papers on equivalent circuits for receiving antennas, we cannot separate these power terms into those due to the transmit coil and those due to the receive coil, and then represent them separately with the corresponding impedances, Z_{11} and Z_{22}. Suppose the incident field is much stronger than the scattered field, and tissue absorption dominates. Then, we have the following approximations:

$$Z_{nn} = \sigma\omega^2\mu^2 A_n^2\, \mathbf{m}_n^\dagger \int \bar{\mathbf{G}}_e^*(\mathbf{x} - \mathbf{x}_n) \cdot \bar{\mathbf{G}}_e(\mathbf{x} - \mathbf{x}_n)\,d\mathbf{x}\,\mathbf{m}_n$$
$$+ R_n - i\omega L_n \qquad n = 1, 2$$

The first part of Z_{11} is the tissue loss resistance when only transmit coil is present, R_1 is the resistance of the transmit coil, and L_1 is its inductance. Similar definitions apply to Z_{22}, R_2, and L_2. The power gain is maximized when the generator impedance Z_G and the load impedance Z_L are conjugate matched to the transceiver equivalent circuit.

Let us consider the same example system as in the previous section. In addition, we define the coil area. To mimic point sources, we choose A_1 and A_2 equal to 4 mm^2 such that impedances Z_{11}, Z_{22}, and Z_{12} can be computed using field expressions derived based on point sources. Furthermore, the wire thickness and the wire width are 0.0381 mm and 0.2032 mm respectively, and the wire conductivity is 59.6×10^6 S/m. Resistances R_n and inductances L_n, $n = 1, 2$, are calculated using formulas from [19]. Fig. 4 plots the variation of the optimal power gain with frequency. The optimal frequencies for both orientations are much sharper. In the face-to-face orientation, the optimal frequency is 2.5 GHz and the corresponding optimal power gain is 0.14 %. In the edge-to-edge orientation, the optimal frequency is 1.6 GHz and the optimal gain is 0.09 %. Note
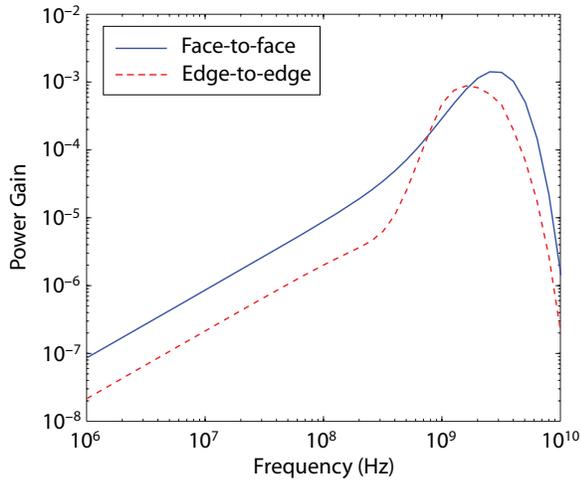
5676

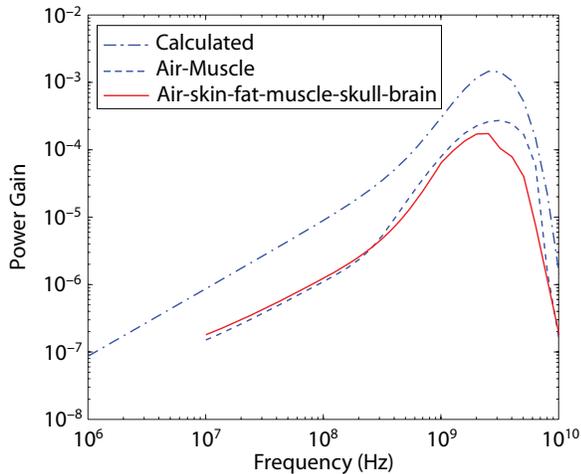Fig. 4. Optimal power gain versus frequency across air-muscle interface.

Fig. 5. Simulation using EM solver with finite coils across air-muscle and air-skin-fat-muscle-skull-brain interfaces.

that these efficiencies are obtained from a pair of single turn 4-mm² coils with separation of 1.5 cm. For the dimension of coils considered in [7], much higher efficiencies can be achieved by operating at the GHz-range than at the MHz-range.

VI. ELECTROMAGNETIC SIMULATIONS

The analytical results and numerical examples presented are based on point sources. We verify the results with finite coils by electromagnetic simulation. We use the electromagnetic solver from Agilent ADS Momentum. We consider two inhomogeneous scenarios: air-muscle interface and air-skin-fat-muscle-skull-brain interface. In the second scenario, the thickness of skin, fat, muscle, and skull are 2 mm, 1 mm, 4 mm, and 8 mm respectively. Square coils of width 2 mm are used. The dimension and conductivity of wire are the same as those in the example system in the previous section. Fig. 5 plots the optimal power gain in the face-to-face orientation. Efficiencies in the two scenarios are similar. The finite-coil efficiencies are approximately 5 dB less than that predicted

from point sources. However, the optimal frequencies are almost the same.

VII. EXPERIMENTS

Two principal obstacles exist to measuring the maximum power gain. First, to directly measure the power gain the link's input and output ports must be conjugately matched to the source and load impedance. Implementing a match which can be tuned over two frequency decades is not possible and to build a distinct match at each measurement frequency would be prohibitively expensive and time consuming. Rather a simpler, and equally accurate approach, is to directly measure the S-parameters of the two port link and from these calculate the maximum power gain, whilst ensuring that the necessary matching components would indeed be feasible.

The second challenge arises in interfacing the very small coil to a network analyzer, and doing so over 2 decades of frequency. If the width between the signal and return lines close to the coil input is large with respect to the coil dimension the transmission parameters will be greatly disturbed at low frequency as that section of the feed line will appear like part of a bigger inductive loop. Therefore the coils cannot directly interface to, for example, a standard SMA to PCB connector for which the pin separation is 4.4 mm. A very low thickness transmission line with characteristic impedance equal to the network analyzer reference impedance is used to simultaneously allow small signal to return line separation at the coil and larger separation signal to return line separation at some distance from the coil in order to minimize interference. Microstrip could not be used as the tissue dielectric constant would be much greater than the board dielectric and thus the characteristic impedance would be highly dependent on the tissue and worse the field about feed line would interfere greatly with the link. The solution was to construct the coil on a 3-layer PCB with controlled dielectric layer thickness of 0.20 mm and to use 50 Ω stripline to feed the coil. At the side of the transmission line closest to the coil the signal line to return line separation is then 0.2 mm, at the side of the stripline furthest from the coil the signal and return traces are spread further apart at 1.5 mm and a custom built narrow PCB to SMA connector is used. Furthermore stripline shields the signal feed so there is minimal interference with the link.

The measurement setup is shown in Fig. 6. We carried out the measurement with beef sirloin. Fig. 7 plots the optimal power gain versus frequency. For reference, it also includes the theoretical curve from Fig. 4 and the simulated curve from Fig. 5. The curves have similar shape and are of approximately the same order of magnitude. At the optimal frequency, around 3 GHz, the measured power gain is about 10 dB better than the simulated one but is close to the power gain derived from point sources.

VIII. CONCLUSIONS

Existing analysis techniques in short-range wireless powering for implantable devices are not adequate to conclude

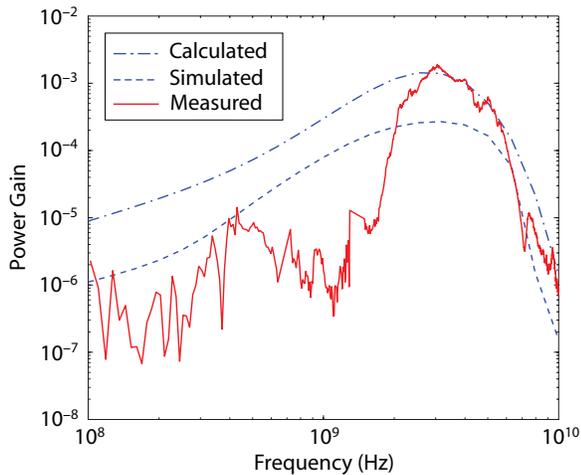**5677**

Fig. 6.   Measurement setup

Fig. 7.   Measurement results

the behavior of power transfer efficiency over a wide frequency range. This paper takes a more vigorous investigation of the variation of power transfer efficiency with frequency from closed-form analyses, electromagnetic simulations to experiments with real biological tissue. It concludes that the optimal operating frequency is at the GHz-range in biological media. In contrast to existing solutions being exclusively in the MHz-range, operating in the GHz-range reduces the size of the receive coil by at least 10^4 times theoretically. This enables us to embed the receive coil in the implant and realize a fully integrated implantable device.

REFERENCES

[1] T. Akin, K. Najafi, and R. M. Bradley, "A wireless implantable multichannel digital neural recording system for a micromachined sieve electrode," *IEEE J. Solid-State Circuits*, vol. 33, no. 1, pp. 109–118, Jan. 1998.

[2] W. Liu, K. Vichienchom, M. Clements, S. C. DeMarco, C. Hughes, E. McGucken, M. S. Humayun, E. de Juan, J. D. Weiland, and R. Greenberg, "A neuro-stimulus chip with telemetry unit for retinal prosthetic device," *IEEE J. Solid-State Circuits*, vol. 35, no. 10, pp. 1487–1497, Oct. 2000.

[3] H. Yu and K. Najafi, "Low-power interface circuits for bio-implantable microsystems," in *Intl. IEEE Solid-State Circuits Conf. (ISSCC)*, San Francisco, CA, Feb. 2003.

[4] J. C. Schuder, H. E. Stephenson, Jr., and J. F. Townsend, "High-level electromagnetic energy transfer through a closed chest wall," *IRE Intl. Conv. Rec*, vol. 9, pp. 119–126, 1961.

[5] J. C. Schuder, J. H. Gold, H. Stoeckle, and J. A. Holland, "The relationship between the electric field in a semi-infinite conductive region and the power input to a circular coil on or above the surface," *Med. Biol. Eng.*, vol. 14, no. 2, pp. 227–234, Mar. 1976.

[6] F. C. Flack, E. D. James, and D. M. Schlapp, "Mutual inductance of air-cored coils: effect on design of radio-frequency coupled implants," *Med. Biol. Eng.*, vol. 9, no. 2, pp. 79–85, Mar. 1971.

[7] W. J. Heetderks, "RF powering of millimeter- and submillimeter-sized neural prosthetic implants," *IEEE Trans. Biomed. Eng.*, vol. 35, no. 5, pp. 323–327, May 1988.

[8] S. F. Pichorim and P. J. Abatti, "Design of coils for millimeter- and submillimetter-sized biotelemetry," *IEEE Trans. Biomed. Eng.*, vol. 51, no. 8, pp. 1487–1489, Aug. 2004.

[9] I. C. Forster, "Theoretical design and implementation of transcutaneous multichannel stimulator for neural prostheses applications," *J. Biomed. Eng.*, vol. 3, pp. 107–120, April 1981.

[10] N. de N. Donaldson and T. A. Perkins, "Analysis of resonant coupled coils in the design of radio-frequency transcutaneous links," *Med. Biol. Eng. Comput.*, vol. 21, pp. 612–627, Sept. 1983.

[11] E. S. Hochmair, "System optimization for improved accuracy in transcutaneous signal and power transmission," *IEEE Trans. Biomed. Eng.*, vol. 31, pp. 177–186, Feb. 1984.

[12] D. C. Galbraith, "An implantable multichannel neural stimulator," Ph.D. dissertation, Stanford University, Dec. 1984.

[13] P. E. K. Donaldson, "Frequency-hopping in R.F. energy-transfer links," *Electron. Wireless World*, pp. 24–26, Aug. 1986.

[14] C. M. Zierhofer and E. S. Hochmair, "High-efficiency coupling-insensitive transcutaneous power and data transmission via an inductive link," *IEEE Trans. Biomed. Eng.*, vol. 37, no. 7, pp. 716–722, July 1990.

[15] A. V. Vorst, A. Rosen, and Y. Kotsuka, *RF/Microwave Interaction with Biological Tissues*.   New Jersey, USA: Wiley-IEEE Press, 2006.

[16] S. Gabriel, R. W. Lau, and C. Gabriel, "The dielectric properties of biological tissues: III. parametric models for the dielectric spectrum of tissues," *Phys. Med. Biol.*, vol. 41, no. 11, pp. 2271–2293, Nov. 1996.

[17] W. C. Chew, *Waves and Fields in Inhomogeneous Media*.   IEEE Press, 1995.

[18] R. E. Collin, "Limitations of the thévenin and norton equivalent circuits for a receiving antenna," *IEEE Antennas Propagat. Mag.*, vol. 45, no. 2, pp. 119–124, April 2003.

[19] T. H. Lee, *The Design of CMOS Radio-Frequency Integrated Circuits*, 2nd ed.   Cambridge University Press, 2003.

5678